

# NUMERICAL AND EXPERIMENTAL STUDY FOR DAMAGE CHARACTERIZATION OF COMPOSITE LAMINATES SUBJECTED TO LOW-VELOCITY IMPACT

Jiangtao Du, Ying Tie\*, Cheng Li, Xihui Zhou

Department of Mechanical Engineering, Zhengzhou University, Zhengzhou 450001, China

\*e-mail: tieying@zzu.edu.cn

**Abstract.** In this paper, the damage evolution and the relationship between damage characterization and impact energy of Carbon/Epoxy composite laminates are discussed. To achieve this purpose, low-velocity impact tests according to ASTM standard are conducted and the data, like impact force, are obtained. Based on ABAQUS / Explicit, a finite element model is established. In the model, the laminate is created by the solid element to better describe the intra-laminar stress and the inter-laminar damage and the cohesive element are introduced to model the interface. By comparing the experiment and simulation, the validity of the simulation is verified. After simulating the impacts with a series of energy values, this paper studies surface pit depth, delamination area and matrix damage area and provides theoretical support for damage research and non-destructive testing.

## 1. Introduction

Composite materials have been widely used in engineering, particularly in the aerospace and automotive industries. Fiber-reinforced composite material is most used in aircraft structure with its unique material properties. This type of composite materials is composed by many single plate layers with different ply angles and the plate layer is made of fibers and matrix [1]. The matrix is mainly responsible for transfer loads and has low strength and toughness, so composite material structure is prone to occur matrix cracking. At the same time, the inter-laminar interface, between the sub-layers which have different ply angles, has low performance, so the structure is also easily to appear delamination damage subject to external loads, especially under impact load.

It's very likely to occur foreign object impact in the process of manufacturing, assembly, use and maintenance of aircraft composite structures, such as collision during transport, drop of maintenance tools and foreign object impact during ups and downs processes. These shocks are mostly low-velocity impact, tend to form smaller pits on the surface, but the inside the material, it has appeared in a large number of delamination and matrix damage [2]. Due to impact damage severely affect the mechanical properties and residual strength of the composite structure, as well as the damage is difficult to find, which increases the harmfulness, it is necessary to study the impact damage's evolution and performance characteristics.

Chio et al. [3] studied composites damage mechanism and influencing factors due to linear impact loads by experiments. They found that matrix cracking firstly appears during the low-velocity impact, and delamination, fiber breakage and other damage are induced by matrix cracking to produce. Haibing Jiang et al. [4] conducted low-velocity impact tests and found that the form of the impact damage and the energy absorption process have the relationship with the impact energy threshold of the material. Morua et al. [5] carried out the low-velocity impact test to carbon/epoxy laminates. It found that the main damage forms subjected to low-velocity impact are delamination and transverse cracks and those forms mutually induce. Zhen et al. [6] found that the damages of composite laminates under two different loads, low-velocity impact and quasi-static indentation (QSI) force, have equivalence and the damage characterization parameters have been compared. F. Caputo et al. [7] established a finite element model of low-velocity impact and analyzed the evolution of injury. H. Yazdani Nezhad et al. [8] carried out tests and simulation analysis, studied the relationship between the damage threshold and the damage area, and presented an accurate modeling approach by comparing the experimental and simulation results. Paul W. Harper et al. [9] studied the influence of the size of the cohesive element to the simulation of delamination and instructed the application of the cohesive element.

In this paper, drop impact tests are conducted to carbon/epoxy composite laminates by ASTM standard [10] and it studies the pit depth, force vs. time curve during the impact and the damage forms. An accurate three-dimensional finite element model is established and its accuracy and reasonableness are verified by comparing with the experimental data. By analyzing the calculations with different impact energies, this paper studies the evolution of the impact damage and uses the pit depths and damage areas can effectively characterize the degree of damage, which can provide theoretical support for non-destructive testing technology.

## 2. Experimental approach

The experimental approach is using the drop impact test, which is conducted by ASTM standard D7136/D7136M-05, shown in Fig. 1.

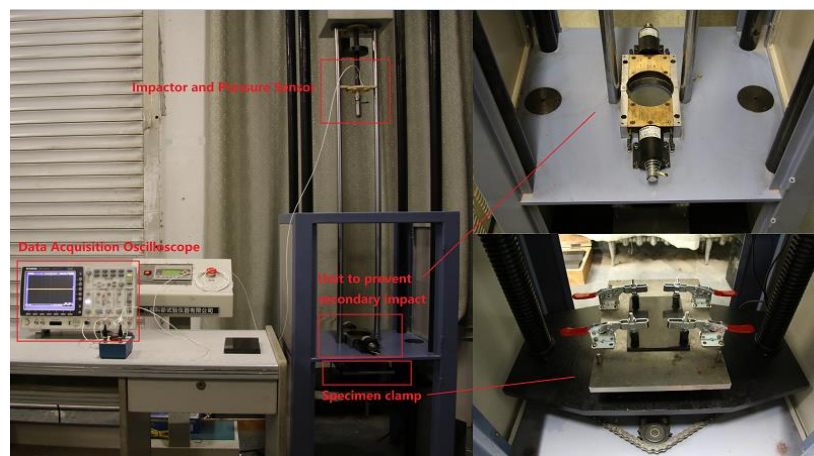


**Fig. 1.** The drop impact test system.

In Figure 1, the left part is a schematic diagram of the test apparatus, which includes the impactor system, the specimen clamp and the data acquisition device. The right part is the

enlarged drawings of the unit preventing secondary impact and the specimen clamp. During the test, the secondary impact may happen, so a photoelectric sensor is placed upon the specimen, which can detect the impactor. When the first impact is done, the unit preventing secondary impact will clamp or catch the impactor.

There is a load cell (PCB 208C05) in the impactor unit, which can measure the pressure up to 34kN, like Figure 2. When the pressure data are achieved, the velocity of the impactor can be calculated by the formulas in the Fig. 2. And the elastic energy and the absorbed energy can also be achieved easily.

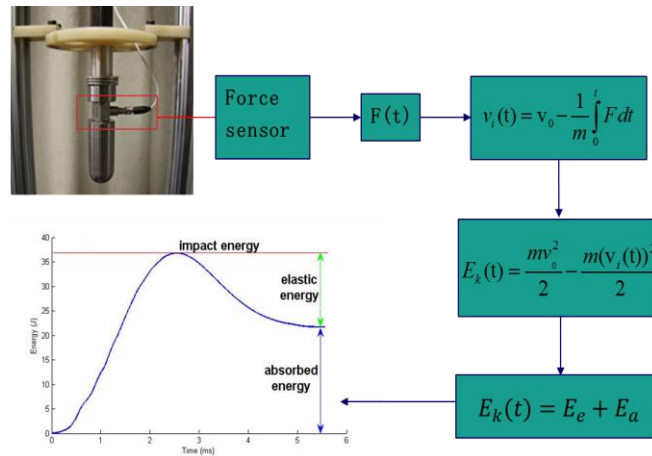


**Fig. 2.** Approach to achieve the energy vs. time curve.

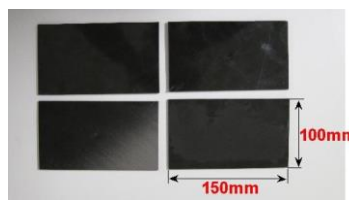


**Fig. 3.** Shape of the laminates.

Table 1. Material properties of the composite laminate.

| Laminate properties     |      | Interfacial properties        |        |
|-------------------------|------|-------------------------------|--------|
| $E_{11}$ (GPa)          | 160  | $G_{IC}$ (N/mm)               | 0.3    |
| $E_{22} = E_{33}$ (GPa) | 9.2  | $G_{IIC}$ (N/mm)              | 0.7    |
| $G_{12} = G_{13}$ (GPa) | 6.2  | $\sigma_{I,max}$ (MPa)        | 30     |
| $G_{23}$ (GPa)          | 3.7  | $\sigma_{II,max}$ (MPa)       | 60     |
| $\nu_{12} = \nu_{13}$   | 0.35 | $K_I$ (N/mm <sup>3</sup> )    | $10^5$ |
| $\nu_{23}$              | 0.4  | $K_{II}$ (N/mm <sup>3</sup> ) | $10^5$ |
| $X_T$ (MPa)             | 1890 |                               |        |
| $X_C$ (MPa)             | 1615 |                               |        |
| $Y_T = Z_T$ (MPa)       | 50   |                               |        |
| $Y_C = Z_C$ (MPa)       | 250  |                               |        |
| $S$ (MPa)               | 105  |                               |        |

The shape of the composite laminates used in the tests is 100 mm in width and 150 mm in length. Each laminate has 24 sub-ply's and each ply's thickness is appropriately 0.15 mm,

so the laminate is 3.6 mm in thickness. The stacking sequence of the laminate is  $(45/-45/90/0)_{3S}$  and the material properties are in Table 1.

In the tests, the impactor has a ball head whose radius is 12.5 mm and the weight of the drop weight is 1.28 kg. Two smooth rails are used to ensure the direction of the impact and it can be considered no energy loss during the fall. So, when the impactor is placed in the height of 1 m, its velocity at the impact time is 4.42 m/s and the impact energy is 12.5 J.

### 3. FE model description

In order to accurately study the stress-strain status and damage conditions during the impact, a three-dimensional finite element model (Fig. 4), consisting of composite laminates, impactor and base, is established. With respect to the laminate, the impactor and the base have greater stiffness, so when the impact is simulated, the impactor and the base can be simplified as rigid bodies. In the laminate model, the approach of refining the central zone is used to ensure the accuracy of the impact simulation and control the size of the model, which can significantly reduce the computation time. The central area has the elements with the size of 1 mm, and the others have the elements with the size of 2.5 mm.

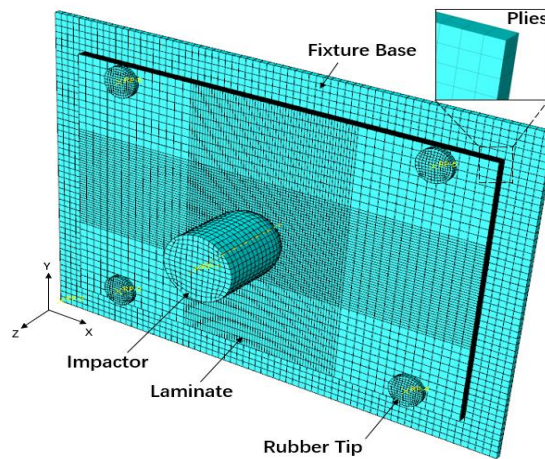


**Fig. 4.** Mesh of the finite element model.

The finite element model of laminates has 24 plies, and each ply, which has one element in the thickness direction, is 0.14 mm. The element type is C3D8R. Among the plies, the cohesive elements with the element type of COH3D8 are created to simulate delamination damage. The cohesive layer also has one element in the thickness direction and its thickness is 0.01 mm. Since delamination occurs only between the plies whose ply angles are different and the difference accelerates the possibility of delamination, so 12 cohesive layers are created only between the plies whose angle difference is  $90^\circ$ .

The finite element model in this paper can be more realistically and accurately simulate the stress and strain conditions of the laminate, but the existing failure criteria and material constitutive model cannot be used in this condition. So basing the ABAQUS/Explicit solver, a user material subroutine (VUMAT) is compiled to solve the problem.

**3.1. VUMAT.** In the process of low-velocity impact to composite laminates, the inter-laminar stress and the shear stress in the thickness direction is very complex and the elements are no longer in the plane stress state, so the solid element is more consistent with the real situation. The subroutine in this paper is based on the three-dimensional Hashin

criterion and its flow chart is in Fig. 5. In the subroutine, four common failure modes are considered, including matrix cracking, matrix compressive failure, fiber tensile failure and fiber compressive failure. And delamination failure is analyzed by the cohesive element which will be described in the section 3.2.

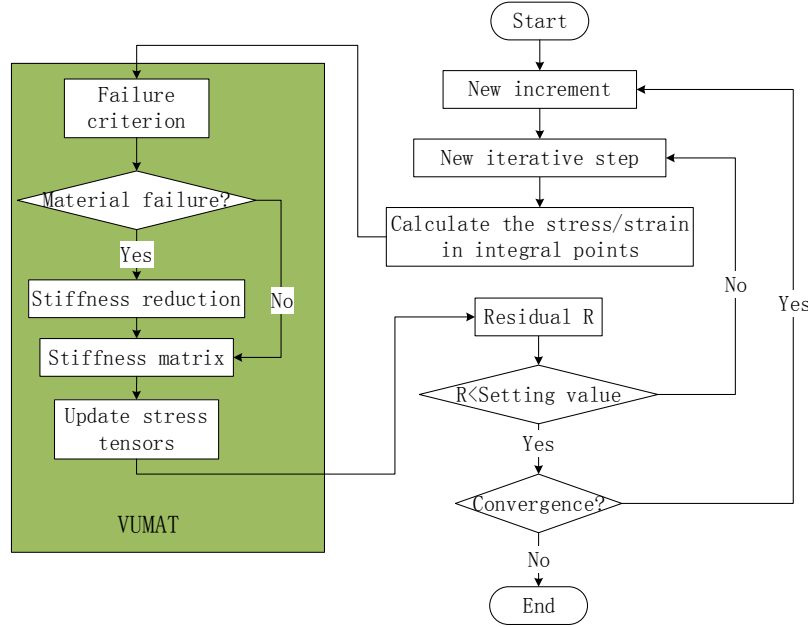


**Fig. 5.** The flow chart of the simulation.

The three-dimensional Hashin criterion applied in the VUMAT is as follows.

**Fiber tensile failure ( $\sigma_{11} \geq 0$ ):**

$$D_{ft} = \left( \frac{\sigma_{11}}{X_t} \right)^2 + \frac{1}{S^2} (\sigma_{12}^2 + \sigma_{13}^2) = 1 \quad \text{or} \quad \sigma_{11} = X_t \quad (1)$$

**Fiber compressive failure ( $\sigma_{11} \leq 0$ ):**

$$D_{fc} = \left( \frac{\sigma_{11}}{X_c} \right)^2 \geq 1 \quad \text{or} \quad |\sigma_{11}| = X_c \quad (2)$$

**Matrix cracking ( $\sigma_{22} + \sigma_{33} > 0$ ):**

$$D_{mt} = \frac{1}{Y_t^2} (\sigma_{22} + \sigma_{33})^2 + \frac{1}{S_t^2} (\sigma_{23}^2 - \sigma_{22}\sigma_{33}) + \frac{1}{S^2} (\sigma_{12}^2 + \sigma_{13}^2) = 1 \quad (3)$$

**Matrix compressive failure ( $\sigma_{22} + \sigma_{33} < 0$ ):**

$$D_{mc} = \frac{1}{Y_c} \left[ \left( \frac{Y_c}{2S_t} \right)^2 - 1 \right] (\sigma_{22} + \sigma_{33}) + \frac{1}{4S_t^2} (\sigma_{22} + \sigma_{33})^2 + \frac{1}{S_t^2} (\sigma_{23}^2 - \sigma_{22}\sigma_{33}) + \frac{1}{S^2} (\sigma_{12}^2 + \sigma_{13}^2) = 1. \quad (4)$$

Wherein  $D_{ft}$ ,  $D_{fc}$ ,  $D_{mt}$  and  $D_{mc}$  are damage coefficients; when their values are 1, it means the element comes to complete failure and when the values are 0, it means there is no damage.

In the after-treatment, it can be used to depict the element state by the output state variables, such as SVD1, SVD2, etc.

During the impact, if the element fails to meet the criteria, the corresponding material stiffness degrades to 0, which means the element loses its carrying capacity. The specific program of the degradation is in Table 2.

Table 2. The degradation program.

| Damage modes               | Degradation criteria |
|----------------------------|----------------------|
| Fiber tensile failure      | $E_1=E_2=G_{12}=0$   |
| Fiber compressive failure  | $E_1=0$              |
| Matrix cracking            | $E_2=0; G_{12}=0$    |
| Matrix compressive failure | $E_2=0; G_{12}=0$    |

**3.2 Cohesive element.** Delamination is the main damage mode of the composite laminates subjected to low-velocity impact and it can be used as an important criterion to evaluate the performance of the laminates. In order to be able to accurately predict the size and position of the delamination, cohesive elements are established between the sub-plyes. The adhesive layer can be seen as a resin-rich region between the fiber plies and contains the pure elastic stage and the softening stage after the yield point.

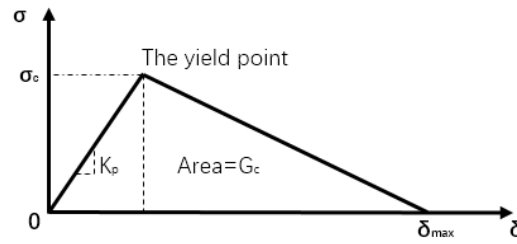


Fig. 6. A typical traction-separation model.

In this paper, the constitutive model of cohesive elements is based on a bilinear traction separation law (Figure 6), relating the inter-laminar stress to the separation displacement, between the nodes at the inter-laminar interface. When the displacement increases, the stress is in a linear increase with slope  $K_p$ , which is the stiffness of the cohesive element. After the stress comes to the maximum, it linearly decreases to zero and at that point, it can be considered that the cohesive element has failed completely and can be deleted. The area surrounded by the stress vs. displacement curve and the horizontal axis is the critical strain energy release rate.

The damage evolution based on fracture energy is used in the modeling approach. Because B-K criterion matches the test data well, so it has been chosen to describe the failure of the cohesive element.

**B-K criterion:**

$$G_{IC} + (G_{IIC} - G_{IC}) \left( \frac{G_{II}}{G_T} \right)^\eta = G_T \quad (5)$$

Wherein  $G_T$  is the critical strain energy release rate of the cohesive element and  $G_T=G_I+G_{II}$ ;  $\eta$  is the material parameter.

## 4. Result and discussion

**4.1. The test results compared with simulation.** In the drop weight impact test, four duplicate experiments with the impact energy 12.5 J are carried out and the front and rear surfaces of the specimens are shown in Fig. 7.

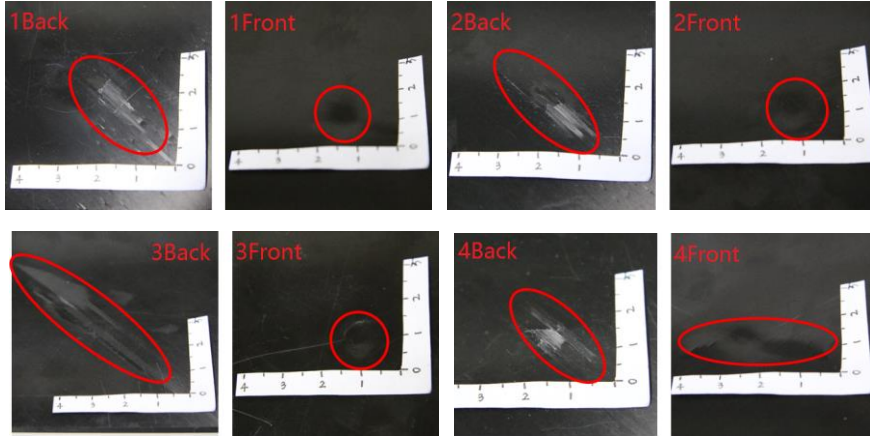


**Fig. 7.** The front and rear surfaces of the specimens.

From the figure, it can be seen that the damage modes of the specimens are consistent and the rear surfaces appear more obvious damage subject to the impact, including matrix cracking, fiber breakage and delamination. The 3rd plate may have internal defects, so more serious matrix cracking and delamination happen. In this case, no fiber breakage occurs. In the front of the plates, a circular dimple-like damage appears with some slight fiber breakage, less obvious. The phenomenon exhibits that the low-velocity impact is hidden and high hazard.

In Figure 8, they are the damage conditions of the front and rear surfaces in the finite element model. The damage modes meet the experiments well: the front of the plate has a circular depression and the rear surface has matrix cracking, fiber breakage and delamination. The adhesive layer, nearest to the lower surface, is chosen to analyze at three different times (Fig. 9). The damage shows double-lobed shape, whose major axis along the fiber direction of the sub-ply away from the impact position [11], namely  $45^\circ$ . By comparison, the finite element model established in this paper analyzes the low-velocity impact well and the simulation matches the test data well. It illustrates the rationality of the subroutine and the correctness of the applications of the cohesive element.

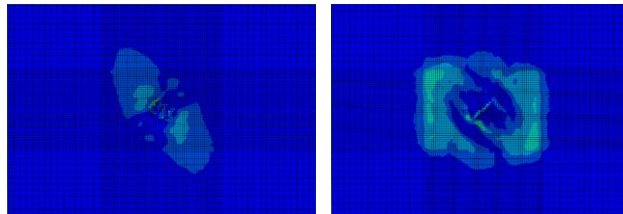


**Fig. 8.** The damage conditions of the simulation.

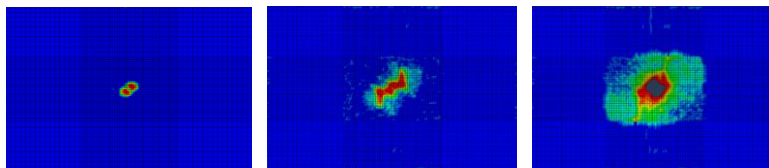


**Fig. 9.** The damage evolution of the adhesive layer.

During the impact, the load force is obtained by the load cell. Using the formulas in Figure 2, the velocity, displacement and energy vs. time curves can also display, shown with the experiment curves in Figure 10, 11, 12, 13. In Figure 10, the force grows stably in the early impact period and can reach 3000 N with the drop weight which is just 1.28 kg. The force vs. time curve is not a smooth one; at 0.5 ms, the force appears the first fluctuation. Compared to the simulation results, it found that matrix cracking occurs at that point. In the later period, the force fluctuates some times and all of them are related to fiber failure and matrix damage.

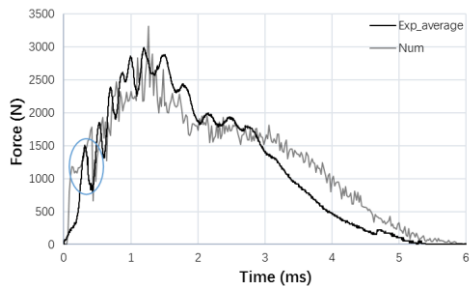


**Fig. 10.** Force vs. time.

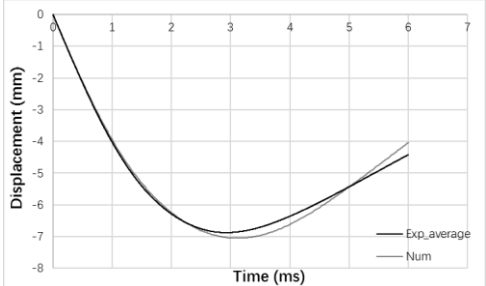


**Fig. 12.** Displacement vs. time.

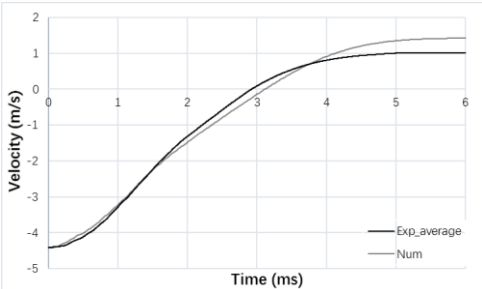


**Fig. 11.** Velocity vs. time.

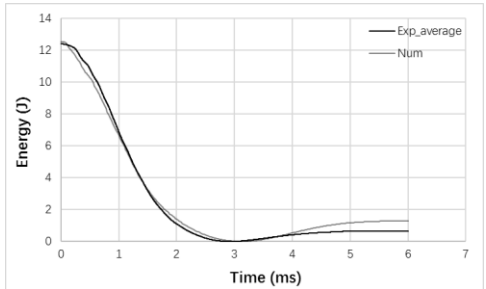


**Fig. 13.** Energy vs. time.

**4.2. Relations between the damage characterization and the impact energy.** By contrasting the drop weight test and the simulation analysis, the model using the subroutine and cohesive element has been verified the accuracy. On this basis, the section analyzes the damage characterizations with different impact energies and discusses relationship between the energy and the damage parameters.

Based on the three-dimensional finite element model mentioned above, ten groups of energy values, from 2.5 J to 25 J, are calculated to study impact damage. Figure 14 is the curve between the pit depth of the laminate and the impact energy. In the case of low-energy impact (less than 7.5 J), the pit depth on the front surface increases slowly with the energy grows; when the impact energy reaches 10 J, the pit depth has a great increase; then, the curve enters a new stable growth stage. Analyzing the simulation result, it can be found that under the energy of 10 J, fiber breakage appears for the first time on the back of the laminate. When the energy comes to 15 J, there are some slight penetration and the pit depth can be considered as the thickness of the laminate and don't increase.

Figure 15 is the delamination area vs. impact energy curve; and Figure 16 is the plate damage area vs. impact energy. The plate damage comprises the matrix damage and the fiber damage. The curves in Figs. 14 and 15 have same growth trend: firstly, it grows slowly; after the point of 7.5 J, fiber breakage occurs and the slope of the curves increases significantly; at the point of 10 J, the delamination area is twice of the area of the 7.5 J. Generally considered



that there is an energy threshold of the damage appearing. Only above it, the impact can cause damage to laminates [12]. Now, it found that for delamination area, there is also a threshold and when the energy is below this value, the delamination area increases slowly. And after that, the delamination area has a great increase. The curve in Fig. 16 has been showing a rising trend and the trend decreases after the penetration occurs.

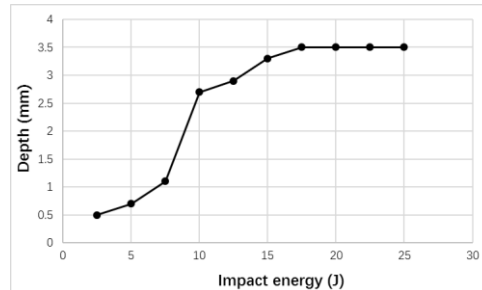


**Fig. 14.** The pit depth vs. impact energy.

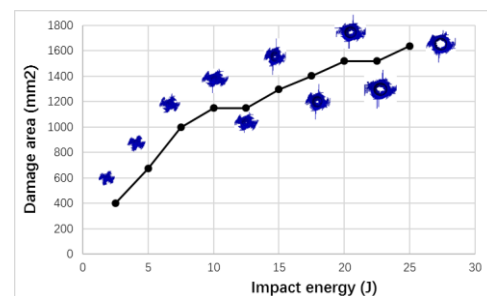
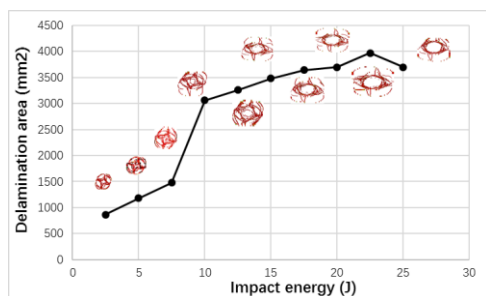


**Fig. 15.** Delamination area vs. impact energy. **Fig. 16.** Damage area vs. impact energy.

For the pit depth, delamination area and plate damage area, the pit depth is a parameter, which is relatively easy to find. In the application process of composite laminates, impact damage is inevitable, but because of the constraint of the various cost, it is impossible to do non-destructive testing for each portion of the composite material structure. So using the pit depth as a preliminary judge of the damage degree is very necessary and reasonable.

## 5. Conclusions

In this paper, the low-velocity impact test and simulation analysis are done to study the generation and evolution of the damage during the impact. Basing on ABAQUS/Explicit solver, an accuracy model created by solid elements is established. In order to describe the damage evolution, a user material subroutine based on 3D Hashin criterion is compiled and the cohesive elements are also created between the sub-ply. By comparison with the experimental data, the simulation results have a high degree of coherency and the modeling approach is reasonable and effective.

Based on the finite element model, this paper studies the damage parameters with different impact energies, including the pit depth of the front surface, the delamination area and the plate damage area. It found that the pit depth and the delamination area has a threshold when they increase with the energy, mainly manifested in the damage parameter has a great increase around the threshold. And using the pit depth as the damage characterization is reasonable, which can be better for the effective detection of the composite structures and timely determine damage caused by low-velocity damage.

### **Acknowledgement**

The authors appreciate their supports from the National Natural Science Foundation of China (U1333201 and 51205370).

### **References**

- [1] G.L. Shen, G.K. Hu, *Composite Mechanics* (Tsinghua University Press, 2006).
- [2] C. Kassapoglou, *Design and Analysis of Composite Structures: With Applications to Aerospace Structures* (John Wiley & Sons Ltd, 2013).
- [3] H.Y. Choi, H.Y.T. Wu, F.K. Chang // *Journal of Composite Materials* **25** (1991) 1012.
- [4] H.B. Jiang, B.R. Wei, Q. Chen, M.Q. Li // *Journal of Aeronautical Materials* **25(3)** (2005) 45.
- [5] M.F.S.F. Moura, A.T. Marques // *Composites Part A: Applied Science and Manufacturing* **33(3)** (2002) 361.
- [6] X.X. Zheng, X.T. Zheng, Z. Shen, S.C. Yang // *Acta Aeronautica Et Astronautica Sinica* **31(5)** (2010) 928.
- [7] F. Caputo, A. De Luca, G. Lamanna, R. Borrelli, U. Mercurio // *Composites Part B: Engineering* **67** (2014) 296.
- [8] H. Yazdani Nezhad, F. Merwick, R.M. Frizzell, C.T. McCarthy // *International Journal of Crashworthiness* **20(1)** (2015) 27.
- [9] P.W. Harper, S.R. Hallett // *Engineering Fracture Mechanics* **75(16)** (2008) 4774.
- [10] ASTM D7136/D7136M-07 standard test method for measuring the damage resistance of a fiber-reinforced polymer matrix composite to a drop-weight impact event, 2003.
- [11] F. Collombet, X. Lalbin, J.L. Lataillade // *Composites Science and Technology* **58** (1998) 463.
- [12] O. Peter, J.T. Hartness, T.M. Cordell // *Computers and Structures* **22** (1988) 30.